Distribution of Crossing Over on Mouse Synaptonemal Complexes Using Immunofluorescent Localization of MLH1 Protein

Lorinda K. Anderson,* Aaron Reeves,* Lisa M. Webb† and Terry Ashley†

**Department of Biology, Colorado State University, Fort Collins, Colorado 80523 and †Department of Genetics, Yale University School of Medicine, New Haven, Connecticut 06510*

Manuscript received September 9, 1998
Accepted for publication December 17, 1998

ABSTRACT

We have used immunofluorescent localization to examine the distribution of MLH1 (*MutL homolog*) foci on synaptonemal complexes (SCs) from juvenile male mice. MLH1 is a mismatch repair protein necessary for meiotic recombination in mice, and MLH1 foci have been proposed to mark crossover sites. We present evidence that the number and distribution of MLH1 foci on SCs closely correspond to the number and distribution of chiasmata on diplotene-metaphase I chromosomes. MLH1 foci were typically excluded from SC in centromeric heterochromatin. For SCs with one MLH1 focus, most foci were located near the middle of long SCs, but near the distal end of short SCs. For SCs with two MLH1 foci, the distribution of foci was bimodal regardless of SC length, with most foci located near the proximal and distal ends. The distribution of MLH1 foci indicated interference between foci. We observed a consistent relative distance (percent of SC length in euchromatin) between two foci on SCs of different lengths, suggesting that positive interference between MLH1 foci is a function of relative SC length. The extended length of pachytene SCs, as compared to more condensed diplotene-metaphase I bivalents, makes mapping crossover events and interference distances using MLH1 foci more accurate than using chiasmata.

MEIOTIC crossing over has been a useful tool to infer the order of genes along chromosomes and to construct genetic linkage maps (*e.g.*, O'Brien 1987). The physical location of meiotic crossovers can be visualized as chiasmata on bivalent chromosomes from diplonema through metaphase I (Brown and Zohary 1955; Jones 1984) or as late recombination nodules (RNs) along synaptonemal complexes (SCs) during pachynema (Carpenter 1975). Even though linkage maps and chiasma/RN maps both reflect crossover events, linkage maps cannot be directly superimposed on corresponding chiasma/RN maps, in part because recombination is not evenly distributed along chromosomes (*e.g.*, Mather 1936; Sherman and Stack 1995; Sybenga 1996).

In general, the pattern of crossover events on chromosomes can be summarized as follows:

1. Ordinarily, each synapsed pair of homologous chromosomes (bivalent) has at least one crossover, regardless of the length of the bivalent (Mather 1936).
2. After the "obligate" crossover, the number of additional exchange events is proportional to chromosomal length; *i.e.*, physically longer chromosomes are more likely to have more than one crossover (*e.g.*, Mather 1936, 1937; Kaback *et al.* 1992).
3. A crossover in one region of a chromosome reduces the likelihood of another crossover nearby (interference, Haldane 1931).
4. Crossovers commonly occur in euchromatin but rarely in heterochromatin (Mather 1939; Wu and Lichten 1994; Sherman and Stack 1995).
5. The frequency and distribution of exchange events often differ between sexes (*e.g.*, between male and female mice, Polani 1972).

While little is known about the bases for these general patterns of crossover distribution, there has been significant progress in understanding the fundamental molecular events of recombination (reviewed by West 1992, 1994; Roeder 1997).

Mapping the physical distribution of crossing over along chromosomes is an important step toward understanding the regulation of crossing over. Many physical maps of recombination have been based on chiasmata, with the most precise maps having been prepared for grasshoppers and locusts, in which diplotene chiasmata are unusually distinct (*e.g.*, Henderson 1963; Fox 1973; Shaw and Knowles 1976; Laurie and Jones 1981). More recently, electron microscopy has been used to visualize and map late RNs on SCs of several organisms (*e.g.*, Carpenter 1975; Zickler 1977; Carmi 1978; Holm and Rasmussen 1980, 1983; Glamann 1986; Sherman and Stack 1995). Although the majority of RN maps have been made using three-dimensional reconstructions of serially sectioned nuclei, SC spreads are much easier to produce and analyze than three-dimensional reconstructions (Rahn and Solari 1986; Stack *et al.*

Corresponding author: Lorinda Anderson, Department of Biology, Colorado State University, Fort Collins, CO 80523.
E-mail: lorrie@lamar.colostate.edu

1993; Pigozzi and Solari 1997). However, late RNs are only rarely observed in SC spreads from mammals (*e.g.*, Poorman *et al.* 1981; Moens *et al.* 1987), so this form of high-resolution physical crossover mapping has not been practical for this group of animals.

An alternative approach for mapping crossover sites on mammalian chromosomes recently became possible using fluorescent immunological detection of MLH1 (*MutL h*omolog) protein on SC spreads. MLH1 is a mismatch repair protein that is similar to the bacterial MutL protein (Bronner *et al.* 1994; Baker *et al.* 1996). Baker *et al.* (1996) proposed that MLH1 protein is involved in reciprocal recombination on the basis of the following evidence: (1) Immunofluorescent localization demonstrated that MLH1 protein was present as discrete foci on pachytene SCs from mice in the approximate frequencies expected for crossing over. (2) Transgenic mice in which MLH1 protein was not expressed had many univalents at metaphase I, even though chromosome synapsis appeared to be normal, suggesting that the defect was not in synapsis but in crossing over. More recently, Hunter and Borts (1997) have provided additional strong evidence that yeast Mlh1 is involved in reciprocal recombination by showing that among several mismatch repair proteins, only Mlh1 promoted crossing over during meiosis. Thus, evidence from both mice and yeast suggests that fluorescent MLH1 foci mark sites of crossing over on mammalian SC spreads. If so, then MLH1 proteins are probably components of late RNs.

Here, we describe the distribution of MLH1 foci on SCs from normal mouse spermatocytes. Although we were not able to identify each autosomal SC with certainty, we defined five size classes of SCs on the basis of relative length, determined the distribution of MLH1 foci on the SCs in each class, and compared the distributions of MLH1 foci to distributions of chiasmata from diplotene-metaphase I bivalents (Polani 1972; Speed 1977; Lawrie *et al.* 1995). For SCs with two foci, the extended length of pachytene SCs enabled us to measure distances between adjacent crossovers on the same SC more accurately than has been possible using condensed diplotene-metaphase I bivalents.

MATERIALS AND METHODS

Mice: Three normal male mice (*Mus domesticus*, inbred strain C57BL), 14–21 days old, were used to prepare SC spreads.

SC spreads: SC spreads were prepared using the technique of Peters *et al.* (1997) with minor modifications. Briefly, both testes were removed from a dead mouse and macerated in ~7 ml of modified Eagle's medium. Large tubules were allowed to settle before the overlying 6 ml of cell suspension was removed and aliquoted equally into six microtubes. The tubes were centrifuged for 5 min at 5800 × *g*. During this time, new slides that had been rimmed on the edges with fingernail polish to make a shallow well were arranged in a level plastic dish that contained a damp paper towel. Sixty-five microliters of an aqueous solution of 1% paraformaldehyde (pH 9.2) and 0.15% Triton X-100 that contained a cocktail of protease inhibitors (final concentration 0.1 μg/ml each for pepstatin A, chymostatin, antipain, and leupeptin, and 1 μg/ml for aprotinin) was dropped onto each slide. The supernatants were removed, and the pelleted cells in each microtube were resuspended in 40 μl of 0.1 m sucrose with the same protease inhibitor cocktail to give a final total volume of 240 μl. A 20-μl aliquot of cell suspension was placed on each of 12 slides, and a cover was placed over the plastic dish so the slides would not dry. After 2 hr, the slides were gently rinsed in 0.4% Photoflo 200 and air dried. Unstained slides were examined using phase microscopy, and only slides on which the cells were well spread were immunostained.

Immunostaining: Immunostaining was performed as described by Moens *et al.* (1987), using a mouse monoclonal antibody to human MLH1 (Pharmingen, San Diego) at 1:100 dilution (Baker *et al.* 1996) and a rabbit antibody to rat SCP3 (a component of lateral elements, 1:1000 dilution, a gift from C. Heyting). Goat anti-mouse rhodamine (Pierce Chemical, Rockford, IL) and goat anti-rabbit fluorescein isothiocyanate (FITC; Pierce) were used at 1:100 dilution. Primary and secondary antibody incubations were 2 hr and 1 hr, respectively. Nuclei were stained with DAPI (2 μg/ml) during the final washing steps.

Fluorescence microscopy and digital image preparation: Slides were examined using a Nikon Eclipse 800 microscope equipped with a black and white CCD camera. Three separate images were taken for each nucleus (MLH1—rhodamine; SCP3—FITC, DAPI). Each image was treated uniformly to reduce background by adjusting levels in Adobe Photoshop (image analysis software). It was necessary to adjust each image because merging three unadjusted images led to a tripling of the background that swamped out the individual signals. The three images were then merged using the GeneJoin Program (Reid *et al.* 1992). The merged images were inverted to facilitate identification of MLH1 foci (white) on SCs (black) or on the DAPI-stained DNA surrounding the SCs (gray shades).

Criteria for analysis of MLH1 distribution on SCs: Each set of SCs included in this analysis met the following two criteria: (1) complete SC sets in which no SCs were broken or obviously stretched and (2) 19 or more MLH1 foci per autosomal SC set. The second criterion is necessary, since immunologically detectable MLH1 foci are transient during pachynema. By setting a lower threshold of 19 foci on the autosomal SCs, each autosome had a chance to have at least one MLH1 focus. Using Moses' (1980) criteria for substaging spreads of SCs at pachynema, most sets with 19 or more foci on the autosomal SCs were from stages PIII (mid pachynema) to PV (late pachynema). MLH1 foci were considered to be on an SC if the two fluorescent signals overlapped.

MLH1 staining background: Spreads of SCs immunostained as usual but lacking MLH1 primary antibody in the first incubation rarely had any foci over nuclei, indicating that there was little nonspecific binding of the secondary antibody. With MLH1 antibody included in the first incubation, MLH1 foci were found regularly on pachytene SCs, but not on zygotene or diplotene SCs. In addition, some MLH1 foci were present on the diffuse chromatin surrounding SCs in nuclei from zygonema through diplonema. On average, the numbers of MLH1 foci over the chromatin (background foci) were not statistically different [analysis of variance (ANOVA), $P > 0.3$] for zygotene, pachytene, or diplotene nuclei. While the foci in the chromatin might represent real concentrations of MLH1 protein, they might also be an indication of the amount of nonspecific "background" staining accompanying the use of this particular primary antibody. Considering sets of SCs with 19 or more total foci, the density of foci on SCs was ~29 times

that on background (0.579 foci/μm^2 *vs.* 0.020 foci/μm^2, n = 47), suggesting that most if not all MLH1 foci detected on SCs are real and not caused by nonspecific background staining of the primary antibody.

To check whether there was any discernible pattern in the location of background foci, we randomly chose 10 nuclei and determined the location of the background foci for the following categories: over euchromatin, over heterochromatin, or close by an SC (within one width of the SC fluorescent signal on either side of the SC). Out of 170 background foci, 71% were over euchromatin, 26% were over heterochromatin, and 3% were close to SCs. The measured surface area of euchromatin averaged 78%, that of heterochromatin averaged 22%, and that defined as close to SC averaged 9%. Therefore, background foci were found over euchromatin and heterochromatin in the approximate proportions expected from their respective surface areas, and background foci were not found disproportionately near SCs.

Measurement procedure: Digital images of MLH1 foci on SC sets were measured using a 32-bit Windows application (http://www.colostate.edu/Depts/Biology/MicroMeasure/). Three measurements of the same set of SCs demonstrated a reproducibility of 0.1 μm in SC length and MLH1 position, which corresponds to 0.8–2.0% of the length of the longest and shortest SCs, respectively.

The position of each MLH1 focus on each SC was recorded as a relative position using distance (percentage of SC length) from the centromere. The centromeric end of each SC was identified by the surrounding AT-rich heterochromatin. After measurement, autosomal SCs in a set were ranked in sequence of decreasing relative length (SCs 1–19). Since there is a continuous gradation in the size of mouse chromosomes (Evans 1989), individual SCs could not be identified unequivocally (Fox 1973; Poorman *et al.* 1981). Therefore, SCs were divided into five classes that included SCs of similar length (SCs 1 and 2, 3–6, 7–12, 13–15, and 16–19). Each SC was divided into 10 equal (10%) length intervals, and MLH1 distributions were obtained by summing the number of foci in each interval for SCs in the same length class.

The relative interference distance between two foci on an SC was determined by converting the relative measured position of each focus to an absolute length position in micrometers on the SC by multiplying the relative position of the focus by the average absolute length of the appropriate SC. The absolute distance between foci was then divided by the average absolute length of euchromatic SC to give relative distances (percentage of euchromatic SC length) between foci. For each SC, euchromatic SC length was determined by subtracting 1 μm (for the length of SC in heterochromatin; Fang and Jagiello 1981; Stack 1984) from the average measured SC length (Table 1).

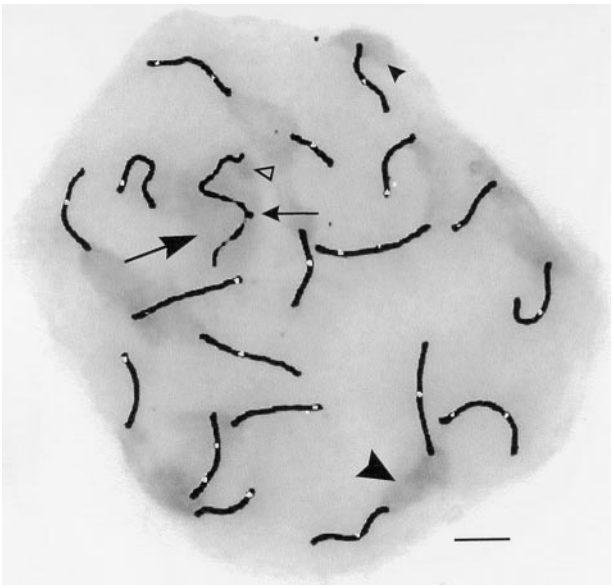

Figure 1.—SC spread from a mouse spermatocyte at pachynema that was immunolabeled with antibodies to SCP3 proteins (black) and MLH1 proteins (white foci). DNA was stained with DAPI (gray). The light gray background is caused by DNA in euchromatin, while the DNA in centromeric heterochromatin appears as a diffuse, darker gray area at one end of each autosomal SC (*e.g.*, small arrowhead) and at the centromeric (nonsynapsed) end of the X (open arrowhead). Often, the centromeric heterochromatin from two or more SCs is associated (*e.g.*, large arrowhead). The heteromorphic sex bivalent is within a darker gray region that corresponds to the sex body (large arrow). There are 24 MLH1 foci of variable size on the SCs and 15 foci on the DAPI-stained chromatin. Many of the background foci cannot be seen clearly because of the loss of contrast in the merging procedure. There is no MLH1 focus on the synapsed, pseudoautosomal region of the XY (small arrow) because the appearance of this focus is not well synchronized with the appearance of maximal numbers of MLH1 foci on autosomal SCs. Using the criteria of Moses (1980) for staging mouse spermatocytes, this nucleus is in stage PIV because 10% or less of the length of the Y is synapsed with the X (small arrow). Bar, 5 μm.

RESULTS

An example of an SC spread from a spermatocyte labeled with antibodies to SCP3 and MLH1 is presented in Figure 1. All mouse autosomes are extreme acrocentrics with blocks of AT-rich heterochromatin around the centromeres (Evans 1989). Because DAPI binds preferentially to AT-rich sequences, the centromeric end of each SC was identified by more intensely stained pericentric heterochromatin. The position of each MLH1 focus was described as a percentage of the SC length measured from the centromere. However, individual SCs in a set were difficult to identify with confidence because the SCs are morphologically uniform and occur in a continuous gradient of lengths (Table 1). As an alternative to trying to identify individual SCs, we divided the SCs into five groups based on similar relative lengths (SCs 1 and 2, 3–6, 7–12, 13–15, and 16–19). Such a classification has three advantages: (1) Different length classes can be more reliably distinguished from one another than individual SCs, particularly if the SC groups being compared are separated by more than one length class (*e.g.*, SCs 1 and 2 compared to SCs 7–12), (2) generalizations can be made about MLH1 focus frequency and distribution with regard to SC length, and (3) SC groups of similar lengths are more likely to coincide with the corresponding chromosome groups identified in the standard mouse idiogram than are individual SCs and chromosomes. This is because individual mitotic chromosomes are identified primarily by their G-banding pattern, so mitotic chromosome

TABLE 1

Average absolute and relative lengths for mouse autosomal SCs (n = 45 SC sets)

SC rank	Average SC length ± SD (μm)	Average % of total autosomal SC length ± SD
1	12.0 ± 1.2	7.3 ± 0.3
2	11.4 ± 1.1	7.0 ± 0.2
3	10.8 ± 1.0	6.6 ± 0.2
4	10.4 ± 1.0	6.3 ± 0.2
5	10.0 ± 0.9	6.1 ± 0.1
6	9.8 ± 0.9	6.0 ± 0.1
7	9.5 ± 0.9	5.8 ± 0.2
8	9.2 ± 0.9	5.6 ± 0.2
9	8.9 ± 0.8	5.4 ± 0.1
10	8.7 ± 0.8	5.3 ± 0.2
11	8.5 ± 0.8	5.2 ± 0.2
12	8.0 ± 0.8	4.9 ± 0.2
13	7.7 ± 0.7	4.7 ± 0.1
14	7.5 ± 0.7	4.6 ± 0.1
15	7.2 ± 0.7	4.4 ± 0.1
16	6.9 ± 0.6	4.2 ± 0.2
17	6.3 ± 0.7	3.8 ± 0.2
18	5.9 ± 0.6	3.6 ± 0.2
19	5.0 ± 0.5	3.0 ± 0.2

numbering does not always correspond to decreasing relative length (*i.e.*, chromosome 12 is longer than chromosome 11; Evans 1989).

During pachynema, the immunological detection of MLH1 foci on SCs was transient. The number of MLH1 foci on autosomal SCs increased gradually from 0 at early pachynema to as many as 27 foci at mid to late pachynema before falling again to 0 at very late stages of pachynema. The sizes of different MLH1 foci in the same nucleus often varied (Figure 1). This size variation could be caused by such factors as (1) differential access of MLH1 proteins to antibodies as a result of the spreading procedure (*e.g.*, if some RNs are below the SCs and less accessible to antibodies than RNs on the top of SCs), (2) a change in the accessibility of MLH1 proteins within the late RNs during pachynema, or (3) a progressive gain then loss of MLH1 proteins at late RNs during mid to late pachynema. Synapsis of the XY pair is delayed relative to the autosomes, but desynapsis of the XY pair precedes desynapsis of the autosomes (Moses 1980). Similarly, the MLH1 focus on the synapsed portion of the XY pair usually appears and disappears during early to mid pachynema, before maximal numbers of MLH1 foci are observed on autosomes at mid- to late pachynema (Figure 1). Because of the transience of MLH1 protein detection and the assumption that there should be at least one MLH1 focus per autosomal SC, only nuclei with at least 19 MLH1 foci on the autosomal SCs were used for analysis. The rationale is that this subset of nuclei should have most, if not all, of the MLH1 foci that will ever be present; thus, an analysis of these nuclei should give the best overall representation of the number and distribution of crossover sites.

Average recombination frequency per spermatocyte: Based on SC sets with 19 or more MLH1 foci, we calculated an average recombination frequency of 22.7 MLH1 foci per set of autosomal SCs in normal mouse spermatocytes (Table 2). This frequency is within the range of the average number of chiasmata per spermatocyte observed for several different strains of mice (22.6–23.9, Table 2).

Average recombination frequency among groups of SCs with different lengths: As expected from previous studies on chiasma frequency per bivalent, short SCs average at least one crossover, and longer SCs have more crossovers on average than shorter SCs (*e.g.*, Mather 1937; Lawrie *et al.* 1995; Table 3).

Distribution of MLH1 foci on SCs: We mapped the distribution of MLH1 foci on 45 sets of SCs (Figure 2). The positions of MLH1 foci on SCs were expressed as a percentage of the SC length from the centromere. This permitted pooling and comparing data from SCs of different lengths. For this, each SC was divided into 10 equal (10%) length intervals, and MLH1 distributions for each SC length class were generated by summing the number of MLH1 foci found in each interval (Figure 2, A–E). However, because the longest mouse SCs are more than twice as long as the shortest (Table 1; Evans 1989), 10% length intervals represent different absolute lengths for different SCs.

For SCs with one MLH1 focus, MLH1 foci were not found in the 10% interval closest to the centromere. The low frequency of foci close to the centromere is probably related to the presence of centromeric heterochromatin on each chromosome. The distributions of single foci along SCs varied among the SC length groups. For the longest SC length groups (SCs 1 and 2 and 3–6), the distributions of MLH1 foci were not significantly different from normal distributions (Kolmogorov-Smirnov test, $P > 0.1$), and both distributions peaked near the middle of the SCs (Figure 2, A and B). For the other SC length groups, the observed distributions were significantly different from normal distributions (Kolmogorov-Smirnov test, $P < 0.002$–0.04). The distribution of single MLH1 foci on SCs 7–12 appeared to be bimodal (Figure 2C), and the distributions of single foci on the shortest SC length groups (SCs 13–15 and 16–19) were skewed toward the telomeres (Figure 2, D and E).

For SCs with two MLH1 foci, there were two peaks of foci with relatively few foci in the intervening region (Figure 2, A–E). Unlike SCs with only one focus, SCs with two foci occasionally had an MLH1 focus in the 10% interval nearest to the centromere (*e.g.*, compare Figure 2, A, C, and D). Even though two MLH1 foci were seldom found on short SCs, when they did occur,

TABLE 2

Average recombination frequency per spermatocyte based on MLH1 foci (this study) or chiasmata (all other references) for different strains of mice

Mouse strain	Number of sets	Average recombination frequency per cell ± SD	Reference
C57BL	45	22.7 ± 2.3[a]	This study
C57BL	872	23.3 (NA)	Speed (1977)
CBA	240	23.9 (NA)	Speed (1977)
Q	792	23.8 (NA)	Speed (1977)
CFLP	100	22.6 ± 1.9	Polani (1972)
AKRT-1	69	23.1 ± 1.7	Polani (1972)
SWISS-CAMM	166	22.6 (NA)	Jagiello and Fang (1979)
C3H/HeH × 101/H	59	23.3 ± 1.8	Lawrie *et al.* (1995)

NA, not available.

[a] Adjusted average that was calculated by taking the counted number of foci per set, subtracting the expected number of background foci per set (0.7), adding the obligate single crossover of the sex bivalent (Hale 1994), and dividing by the total number of sets analyzed.

one tended to lie nearer to the centromere and the other near the distal telomere (Figure 2, D and E).

Only four SCs (ranked by length as SCs 1, 3, 4, and 5) in four different SC sets were observed with three foci. For the SC 1 with three foci, the proximal and distal foci were no closer to the centromere or telomere, respectively, than the most proximal and distal foci observed on other SCs 1 with single or double foci. For the other three SCs with three foci (SCs 3–5), however, either the most proximal (SCs 4 and 5) or the most distal (SC 3) focus was closer to the centromere or telomere, respectively, than was observed for any other SCs 3–5.

All SC length groups have a large proportion of MLH1 foci located near the telomeres (Figure 2). When the bivalents were subdivided into 5% length intervals, however, the highest level of recombination was not in the most distal telomeric segment, but in the subtelomeric 91–95% interval, where almost 14% of all foci occurred (Table 4).

Distance between two foci on the same SC: When two foci were present on the same SC, the foci were usually separated by a substantial proportion of the SC length (Figure 2; Table 5). Since the observed average separation between two foci (59–65% of the euchromatic SC length) is substantially greater than the expected average separation between two randomly placed foci (33% of euchromatic SC length), crossover interference seems to affect the placement of pairs of MLH1 foci. The average absolute distance between two foci varied from 3 to 7 μm, depending on the SC length group. Thus, even though there is a 1.7-fold difference in absolute SC length between SCs 1 and 15, the average relative distance between two foci was not significantly different for any of the SC length groups (except for the shortest SC length group that was excluded because of the low number of observations; ANOVA, $P > 0.9$).

DISCUSSION

Correspondence between the frequency of chiasmata and MLH1 foci: The average number of MLH1 foci that we observed in mouse primary spermatocyte nuclei with 19 or more foci (~23) is comparable to the average number of chiasmata that have been observed in spermatocytes from a variety of different mouse strains (Ta-

TABLE 3

Average number of MLH1 foci and frequency of SCs with zero to three MLH1 foci for SCs of different length classes (n = 45 sets)

SC rank	Total no. SCs observed	Average no. of MLH1 foci ± SD	Frequency (%) of SCs with			
			No foci	One focus	Two foci	Three foci
SCs 1 and 2	90	1.42 ± 0.54	1	57	41	1
SCs 3–6	180	1.38 ± 0.54	1	62	36	2
SCs 7–12	270	1.19 ± 0.48	4	74	23	0
SCs 13–15	135	0.99 ± 0.40	8	84	7	0
SCs 16–19	180	0.97 ± 0.31	6	91	3	0
All SCs	855		4	75	21	<1

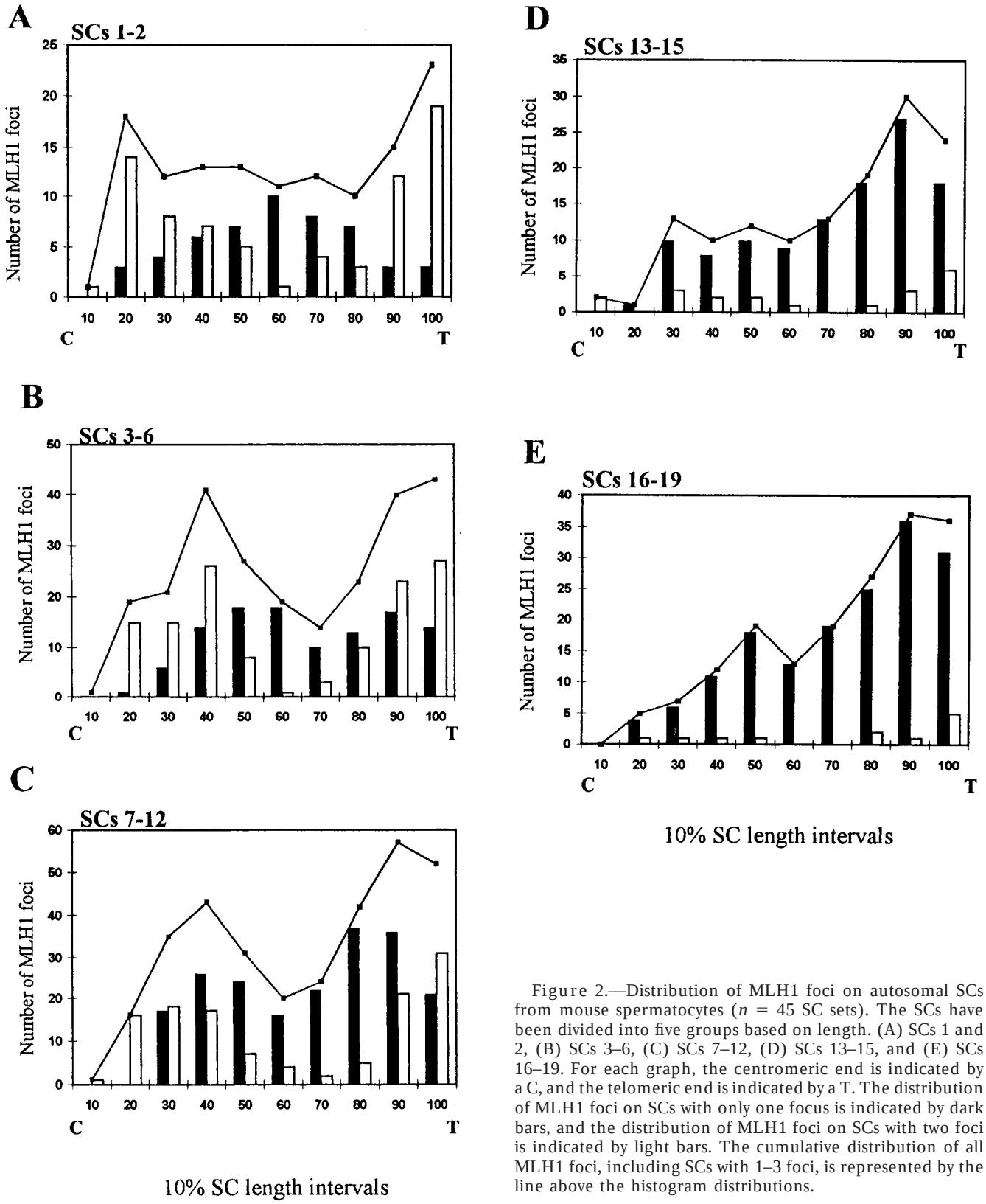

Figure 2.—Distribution of MLH1 foci on autosomal SCs from mouse spermatocytes (n = 45 SC sets). The SCs have been divided into five groups based on length. (A) SCs 1 and 2, (B) SCs 3–6, (C) SCs 7–12, (D) SCs 13–15, and (E) SCs 16–19. For each graph, the centromeric end is indicated by a C, and the telomeric end is indicated by a T. The distribution of MLH1 foci on SCs with only one focus is indicated by dark bars, and the distribution of MLH1 foci on SCs with two foci is indicated by light bars. The cumulative distribution of all MLH1 foci, including SCs with 1–3 foci, is represented by the line above the histogram distributions.

ble 2). The shorter SCs usually have 1 MLH1 focus, while the longer SCs average more than 1 focus. This is consistent with previous studies that have reported a positive correlation between chromosome length and number of crossovers (*e.g.*, Mather 1936, 1937; Lawrie *et al.* 1995). Most mouse SCs have 1 or 2 MLH1 foci, but occasional SCs with 3 or 0 foci were observed (0.5 and 4% of all SCs, respectively). Similarly, most diplotene-

TABLE 4

Frequency of MLH1 foci observed in each 5% SC length interval (starting from the centromere) for all 19 autosomal SCs of normal mice (n = 45 sets of SCs)

SC length intervals (%)	Frequency of foci (%)		
	Only SCs with one focus	Only SCs with two foci	SCs with one to three foci
0–5	0.0	0.6	0.2
5–10	0.0	0.6	0.3
10–15	0.6	6.5	3.0
15–20	0.8	6.5	2.9
20–25	1.6	7.0	3.5
25–30	5.2	5.6	5.3
30–35	5.2	8.4	6.3
35–40	5.0	6.5	5.6
40–45	6.1	4.8	5.7
45–50	6.0	1.7	4.5
50–55	5.2	0.8	3.6
55–60	5.2	1.1	3.7
60–65	5.2	1.1	3.8
65–70	6.1	1.4	4.4
70–75	8.2	3.9	6.6
75–80	7.5	2.0	5.5
80–85	8.6	8.4	8.4
85–90	10.0	8.4	9.3
90–95	11.1	18.5	13.7
95–100	2.5	6.2	4.0
Total	100.1	100.0	100.3
Total no. of foci	638	356	1006

metaphase I bivalents from male mice have been reported to have one or two chiasmata, but rarely three (Speed 1977; Jagiello and Fang 1979; Lawrie *et al.* 1995). Speed (1977) and Jagiello and Fang (1979) also observed that 2–4% of normal mouse spermatocytes had univalents at diplotene and that univalents were more likely among short chromosomes than among long chromosomes. This is consistent with our observation that among SC sets with 19 or more MLH1 foci, there were no foci on 4% of autosomal SCs and most of the SCs without foci were short (Table 3).

Despite the similarity in the frequency of univalents determined by chiasma studies and MLH1 foci, it is possible that some of the SCs that we observed with no foci (or 1 rather than 2 foci) resulted from the transient immunological detection of MLH1. During pachynema, the number of MLH1 foci on autosomal SCs increased gradually to as many as 27 foci at mid to late pachynema before gradually falling again to 0 at very late stages of pachynema. It is not clear whether MLH1 proteins were not present in foci at these later stages, or if MLH1 proteins were still present but no longer detectable with antibodies. In any case, the close correspondence between the frequency and distribution of crossovers determined from MLH1 foci and chiasmata (see below) indicates that the transiency of MLH1 foci had little effect on our results.

Correspondence between distribution of chiasmata, MLH1 foci, and crossing over: Previous studies by Polani (1972) and Speed (1977) on chiasma distribution in spermatocytes showed that most chiasmata were located distally. Because of the difficulty of identifying individual mouse chromosomes, these investigators simply divided each chromosome into three segments (proximal, central, and distal) to describe the general location of chiasmata and the frequency of different chiasma configurations. More recently, Lawrie *et al.* (1995) described chiasma distribution patterns for both male and female mice in more detail by ranking each bivalent according to relative length and graphing the distribution of chiasmata along the bivalents. Lawrie *et al.* (1995) found that the distributions of chiasmata for male mice fell into one of two patterns: (1) For longer bivalents that often had two chiasmata, the distribution of chiasmata was bimodal with peaks at the proximal and distal ends of the bivalents. (2) For shorter bivalents that usually had only a single chiasma, there was a single major peak of chiasmata located at the distal end. Because of uncertainty in accurately identifying individual bivalents using only relative length (Fox

TABLE 5

Mean distances between two MLH1 foci for mouse SCs of different length groups

SC length group	No. observed	Distance between two foci (μm)		Relative distance between two foci (% euchromatic SC length)	
		Average ± SD	Range	Average ± SD	Range
SCs 1 and 2	37	7.0 ± 1.7	2.7–10.0	65.3 ± 15.4[a]	26–91
SCs 3–6	64	5.9 ± 1.4	2.6–8.9	63.3 ± 15.4[a]	28–93
SCs 7–12	61	5.1 ± 1.5	0.8–7.7	64.6 ± 18.9[a]	10–91
SCs 13–15	10	4.2 ± 1.0	2.5–5.8	65.2 ± 15.4[a]	38–90
SCs 16–19	6	3.1 ± 1.6	0.9–4.4	58.5 ± 31.4[b]	18–99

[a] Not significantly different, ANOVA, $P > 0.9$.
[b] Not included in ANOVA test because <10 observations.

1973; Poorman *et al.* 1981), we chose to group mouse SCs into different length classes. Even so, the general patterns of chiasma distributions that Lawrie *et al.* (1995) obtained for bivalents of different lengths correspond to the patterns of MLH1 foci distribution that we observed (compare their Figure 3 with our Figure 3). One difference, however, is that we did not observe peaks of MLH1 foci at the extreme proximal and distal ends of bivalents, as reported by Lawrie *et al.* (1995). Instead, the peaks of MLH1 foci we observed occurred subterminally on SCs, immediately distal to the centromeric heterochromatin and/or immediately proximal to the telomere (Figure 2; Table 4). It is likely that recombination at either of these subterminal locations would give rise to chiasmata that would appear terminal in more condensed diplotene-metaphase I bivalents. These observations also demonstrate the higher resolution of MLH1 foci compared to chiasmata for mapping purposes.

Glamann (1986) described the location of recombination nodules/bars along mouse SCs using three-dimensional electron microscopic reconstructions of spermatocyte nuclei. Glamann (1986) also grouped SCs by length, although he made four length groups compared to our five. On the basis of 13 reconstructions of mid- to late pachytene nuclei, Glamann (1986) found an average of only 14 RNs per nucleus compared to an average of ~23 MLH1 foci and chiasmata that we and others have observed. Even so, the general form of the distributions of RNs/bars along SCs that Glamann (1986) observed was similar to our results for different SC length groups.

Variation in frequency of crossing over along mouse chromosomes has also been observed using genetic markers (Lyon 1976; Nachman and Churchill 1996). Similar to the results from MLH1 foci and chiasmata, centromeric regions have relatively low recombination rates, while telomeric regions have higher recombination rates.

With the demonstration that MLH1 foci accurately mark crossover sites, exchange events can now be mapped on mouse SCs in unusual situations, such as meiocytes that do not progress beyond pachynema (*e.g.*, X-A translocations; de Boer and de Jong 1989) and chromosomal aberrations that are difficult to interpret using chiasmata (*e.g.*, heterozygous inversions; Sybenga 1975). In addition, MLH1 foci could be used to assess the influence of various meiotic mutations on recombination in transgenic mice.

Patterns of MLH1 distribution on mouse SCs: The pattern of distribution of single foci on SCs was dependent on the length of the SCs. In general, the longer the mouse SCs, the greater the likelihood that a single MLH1 focus will be near the center of the SC. Conversely, the shorter the mouse SCs, the greater the likelihood that a single MLH1 focus will be closer to the distal telomere. The different distributions of single foci for short and long acrocentric mouse chromosomes may be related to synaptic initiation patterns, the centromere effect, and/or interference (see below). In contrast to the distribution of single MLH1 foci, which varied according to SC length, the distributions of two foci on SCs of all lengths appeared to be bimodal, probably because of crossover interference. Similar observations regarding the distributions of single and double crossovers have been made for a number of organisms (*e.g.*, Charles 1938; Stephens 1961; Lindsley and Sandler 1977; also see Jones 1984 and Carpenter 1988 for reviews).

Interference distances between two MLH1 foci on the same SC: The minimum distance observed between two foci on the same mouse SC was 0.8 μm (Table 5). Sherman and Stack (1995) found late RNs as close together as 0.3 μm on tomato SCs. These observations indicate that interference does not always block closely adjacent crossovers. The maximum distance between two foci on the same mouse SC approached 85% of total SC length and up to 99% of euchromatic SC length (Table 5). Thus, foci can be as far apart as possible in the euchromatic segments of the chromosomes, but they are typically excluded from the centromeric heterochromatin that accounts for 10–20% of the length of each mouse SC (Fang and Jagiello 1981; Stack 1984; our observations). This result was expected on the basis of the general suppression of crossing over in centromeric heterochromatin (*e.g.*, Mather 1939).

The average absolute distance between two MLH1 foci on one SC ranged from ~3 to 7 μm, depending on the SC length class (Table 5). When expressed as a percentage of euchromatic SC length, however, the average distance between two MLH1 foci was not significantly different for any of the SC length classes that often had two foci, *i.e.*, SCs 1–12 (Table 5). Sherman and Stack (1995) made similar observations for pairs of RNs on tomato SC arms of different lengths, and comparable observations have been made regarding the relative positions of two chiasmata on bivalents of different lengths for locusts (Henderson 1963) and humans (Hulten 1974).

The observed distributions of relative distances between pairs of MLH1 foci on the euchromatic portion of the 8 longest mouse SCs, between pairs of RNs on the euchromatic portion of the long arms of the 12 SCs of tomato (Sherman and Stack 1995), and between pairs of RNs on acrocentric ZW SCs of the bird *Rhea americana* (Pigozzi and Solari 1997) are shown in Figure 3, along with the expected distribution of distances if pairs of foci were located randomly and independently along SCs. Segments of the curves that fall below the expected line indicate positive crossover interference, while segments of the curves that rise above the expected line are defined as negative crossover interference (*i.e.*, a high likelihood of occurrence). For mouse acrocentric chromosomes, there is almost complete positive interference between MLH1 foci up to 40% of

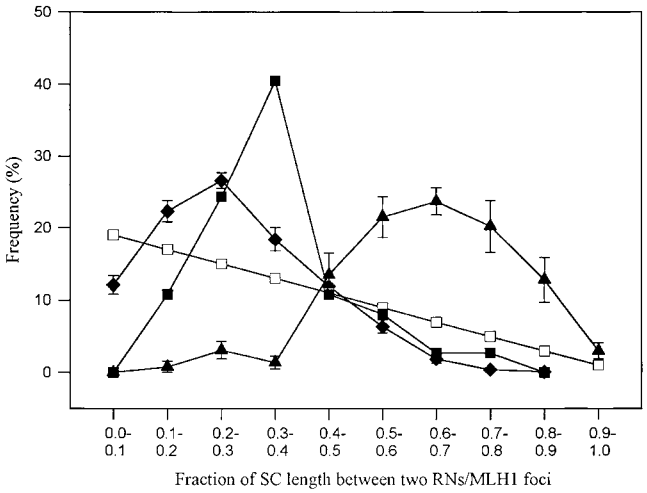

Figure 3.—Expected (open squares) and observed distributions of relative SC distance between MLH1 foci or RNs on the 8 longest autosomal SCs of the mouse (n = 162, solid triangles), the 12 tomato SCs (n = 1690, solid diamonds, data from Sherman and Stack 1995), and the acrocentric ZW bivalents of the bird *Rhea americana* (n = 37, solid squares, data from Pigozzi and Solari 1997). The data are limited to SC long arms that have only two MLH1 foci or RNs and to SCs for which there are at least 10 observations. Because of the latter restriction, the data from the mouse are limited to the eight longest SCs. The distance between two foci and RNs is expressed as a percentage of SC length (Rhea) or euchromatic arm length (mouse and tomato). The expected distribution is based on random and independent location of two RNs on an SC according to Sherman and Stack (1995). Error bars (standard error of the mean) are given for the mouse and tomato observations, but not for Rhea, because observations from only ZW bivalents were given by Pigozzi and Solari (1997). Using the Kolmogorov-Smirnov goodness-of-fit test, the distributions for tomato, mouse, and Rhea are all significantly different from one another (mouse *vs.* tomato, $P < 0.01$; mouse *vs.* Rhea, $P < 0.01$; tomato *vs.* Rhea, $P < 0.05$). Observations of distance between two MLH1 foci or RNs below the expected line indicate positive crossover interference, while distances between MLH1 foci or RNs higher than the expected line indicate negative interference (*i.e.*, a high likelihood of occurrence; Sherman and Stack 1995).

the euchromatic SC length. Positive interference then rapidly decreases and crosses into negative interference at ~49% of euchromatic SC length. Negative interference then peaks at a separation distance of 60–70% of euchromatic SC length. The distributions of inter-RN distances for tomato and Rhea SCs show a similar pattern to that of the mouse in that they have positive interference at short separation distances followed by negative interference at longer separation distances. The extent of positive interference between RNs in tomato and Rhea (~17 and 24% of SC length, respectively), however, is not as great as in the mouse, nor does negative interference extend as far as in the mouse. For tomato and Rhea, but not for the mouse, there seems to be a reimposition of positive interference once RNs are separated by 60% of SC length, but whether the "positive interference" at longer separation distances is related to positive interference at short separation distances is unclear. Similar patterns of interference (positive interference followed by negative interference) have been observed for the long arm of the L3 bivalent in the grasshopper *Chorthippus brunneus* (Laurie 1980 as cited by Jones 1984) and for the acrocentric X chromosome of Drosophila (Charles 1938; Stephens 1961; Carpenter 1988). Indeed, Carpenter (1988) suggested that this basic pattern of interference may be universal.

In summary, the results from tomato, Rhea, and mouse suggest that positive interference between two RNs or two MLH1 foci is a function of relative, not absolute, SC length, and that positive interference operates over different relative distances in different organisms.

Control of MLH1 distribution: Several factors, including synaptic initiation patterns, centromere effect, and interference, apparently influence the distribution of MLH1 foci on mouse SCs. There are many observations that segments of chromosomes which synapse first (usually distal ends) tend to cross over more often (see Jones 1984 for a review and subsequently Stack and Anderson 1986; Zickler *et al.* 1992). Synapsis in the mouse usually begins distally (Dietrich and de Boer 1983; Guitart *et al.* 1985; Scherthan *et al.* 1996), and we found more MLH1 foci in this region of SC than in any other (Figure 2). Synapsis can also begin interstitially, particularly for longer SCs that tend to have more synaptic initiation sites than shorter SCs (Dietrich and De Boer 1983; Guitart *et al.* 1985; Scherthan *et al.* 1996; our unpublished observations). For individual autosomes, the MLH1 distributions that we observed could be affected by the relative probabilities of distal compared to interstitial synaptic initiation. For example, one explanation for the pattern of single and double foci on the long SCs 1 and 2 could be that synapsis often initiates near the distal telomeres, and, as a result, a crossover is more probable at that location. Because the first crossover is so close to one end, there is enough remaining SC length for positive crossover interference to dissipate sufficiently for a second crossover to occur at ~60% of the SC length from the first crossover. If a distal crossover does not occur first, possibly because synapsis initiated interstitially, then the initial crossover may occur near the middle of the SC, where interference extending in either direction can prevent a second crossover. For shorter SCs, the distal clustering of MLH1 foci could be caused by a tendency for synapsis to begin first distally along with suppression of more proximal crossovers by the centromere effect or undiminished crossover interference.

Crossover distribution is also influenced by chromosome structure, as shown by the lack of MLH1 foci on mouse SCs in pericentric heterochromatin. In addition, each mouse chromosome has a unique G-banding pattern that may affect crossover distribution (Chandley

1986). For mouse chromosomes, euchromatic R-bands are interspersed with G-bands that are considered to be facultative heterochromatin (Holmquist 1989). Since chromatin conformation is an important factor controlling crossovers (Wu and Lichten 1994), the more open chromatin configuration at R-bands may provide preferred sites for synaptic initiation and/or crossing over (Chandley 1986; Ashley 1988).

To date, there is no detailed information regarding the patterns of synaptic initiation and crossover (MLH1) distribution for individual mouse chromosomes. In the future, however, combining immunological localization of SC and MLH1 proteins with *in situ* hybridization to identify specific chromosomes (*e.g.*, Heng *et al.* 1994; Rabbits *et al.* 1995; Barlow and Hulten 1996) may permit a more detailed assessment of the influence of synapsis and chromatin type on crossover distribution.

Crossover interference also influences MLH1 distribution. Although the basis for interference is unknown, there is a growing consensus that the SC is involved in transmission of the interference signal (Sym and Roeder 1994; Egel 1995; Roeder 1997; but see Herickhoff *et al.* 1993; Kleckner 1996). Models to explain interference generally fall into two classes. One class proposes that interference diminishes over physical distance (*e.g.*, Henderson 1963; Fox 1973; King and Mortimer 1990), while the other proposes that interference is a function of genetic distance (Foss *et al.* 1993). Our data suggest that crossover interference is a combined function of absolute SC length (longer SCs have more crossovers) as well as relative SC length (if two crossovers occur on an SC they are usually separated by a characteristic percentage of the SC length). These observations are not readily explained by current models for interference.

We thank Christa Heyting (Wageningen Agricultural University) for providing antibodies to SCP3, Stephen Stack (Colorado State University), Hans de Jong (Wageningen Agricultural University) and two anonymous reviewers for helpful comments on the manuscript, and Jim Zumbrunnen (Colorado State University) for assistance with statistics. Financial support for A. Reeves was provided by Colorado Agricultural Experiment Station grant COL00624 to Stephen Stack (Colorado State University). This work was supported by National Institutes of Health grant GM-49779 to T.A.

LITERATURE CITED

Ashley, T., 1988 G-band position effects on meiotic synapsis and crossing over. Genetics **118:** 307–317.

Baker, S. M., A. W. Plug, T. A. Prolla, C. E. Bronner, A. C. Harris *et al.*, 1996 Involvement of mouse *Mlh1* in DNA mismatch repair and meiotic crossing over. Nat. Genet. **13:** 336–342.

Barlow, A. L., and M. A. Hulten, 1996 Combined immunocytogenetic and molecular cytogenetic analysis of meiosis I human spermatocytes. Chrom. Res. **4:** 562–573.

Bronner, C. E., S. M. Baker, P. T. Morrison, G. Warren, L. G. Smith *et al.*, 1994 Mutation in the DNA mismatch repair gene homologue *hMLH1* is associated with hereditary non-polyposis colon cancer. Nature **368:** 258–261.

Brown, S. W., and D. Zohary, 1955 The relationship of chiasmata and crossing over in *Lilium formanosum.* Genetics **40:** 850–873.

Carmi, P., P. B. Holm, Y. Koltin, S. W. Rasmussen, J. Sage *et al.*, 1978 The pachytene karyotype of Schizophyllum commune analyzed by three dimensional reconstruction of synaptonemal complexes. Carlsberg Res. Commun. **43:** 117–132.

Carpenter, A. T. C., 1975 Electron microscopy of meiosis in *Drosophila melanogaster* females. II. The recombination nodule—a recombination-associated structure at pachytene? Proc. Natl. Acad. Sci. USA **72:** 3186–3189.

Carpenter, A. T. C., 1988 Thoughts on recombination nodules, meiotic recombination, and chiasmata, pp. 529–548 in *Genetic Recombination*, edited by R. Kucherlapati and G. R. Smith. American Society of Microbiology, Washington, DC.

Chandley, A. C., 1986 A model for effective pairing and recombination at meiosis based on early replicating sites (R-bands) along chromosomes. Hum. Genet. **72:** 50–57.

Charles, D. R., 1938 The spatial distribution of crossovers in X-chromosome tetrads of *Drosophila melanogaster*. J. Genet. **36:** 103–126.

de Boer, P., and J. H. de Jong, 1989 Chromosome pairing and fertility in mice, pp. 37–76 in *Chromosome Pairing: Recent Studies in Plants and Animals*, edited by C. B. Gillies. CRC Press, Boca Raton, FL.

Dietrich, A. J. J., and P. De Boer, 1983 A sequential analysis of the development of the synaptonemal complex in spermatocytes of the mouse by electron microscopy using hydroxyurea and agar filtration. Genetica **61:** 119–129.

Egel, R., 1995 The synaptonemal complex and the distribution of meiotic recombination events. Trends Genet. **11:** 206–208.

Evans, E. P., 1989 Standard normal chromosomes, pp. 576–578 in *Genetic Variants and Strains of the Laboratory Mouse*, edited by M. P. Lyon and A. G. Searle. Oxford University Press, Oxford.

Fang, J. S., and G. Jagiello, 1981 A pachytene map of the mouse spermatocyte. Chromosoma **82:** 437–445.

Foss, E., R. Lande, F. W. Stahl and C. M. Steinberg, 1993 Chiasma interference as a function of genetic distance. Genetics **133:** 681–691.

Fox, D. P., 1973 The control of chiasma distribution in the locust, *Schistocerca gregaria* (Forskal). Chromosoma **43:** 289–328.

Glamann, J., 1986 Crossing over in the male mouse as analysed by recombination nodules and bars. Carlsberg Res. Commun. **51:** 143–162.

Guitart, M., M. D. Coll, M. Ponsa and J. Egozcue, 1985 Sequential study of synaptonemal complexes in mouse spermatocytes by light and electron microscopy. Genetica **67:** 21–30.

Haldane, J. B. S., 1931 The cytological basis of genetical interference. Cytologia **3:** 54–64.

Hale, D. W., 1994 Is X-Y recombination necessary for spermatocyte survival during mammalian spermatogenesis? Cytogenet. Cell Genet. **65:** 278–282.

Henderson, S. A., 1963 Chiasma distribution at diplotene in a locust. Heredity **18:** 173–190.

Heng, H. H. Q., L-C. Tsui and P. B. Moens, 1994 Organization of heterologous DNA inserts on the mouse meiotic chromosome core. Chromosoma **103:** 401–407.

Herickhoff, L., S. Stack and J. Sherman, 1993 The relationship between synapsis, recombination nodules and chiasmata in tomato translocation heterozygotes. Heredity **71:** 373–385.

Holm, P. B., and S. W. Rasmussen, 1980 Chromosome pairing, recombination nodules, and chiasma formation in diploid *Bombyx* males. Carlsberg Res. Commun. **45:** 483–548.

Holm, P. B., and S. W. Rasmussen, 1983 Human meiosis VI. Crossing over in human spermatocytes. Carlsberg Res. Commun. **48:** 385–413.

Holmquist, G. P., 1989 Evolution of chromosome bands: molecular ecology of noncoding DNA. J. Mol. Evol. **28:** 469–486.

Hulten, M., 1974 Chiasma distribution at diakinesis in the normal human male. Hereditas **76:** 55–78.

Hunter, N., and R. H. Borts, 1997 Mlh1 is unique among mismatch repair proteins in its ability to promote crossing-over during meiosis. Genes Dev. **11:** 1573–1582.

Jagiello, G., and J. S. Fang, 1979 Analyses of diplotene chiasma frequencies in mouse oocytes and spermatocytes in relation to ageing and sexual dimorphism. Cytogenet. Cell Genet. **23:** 53–60.

Jones, G. H., 1984 The control of chiasma distribution, pp. 293–320 in *Controlling Events in Meiosis*, edited by C. Evans and H. Dickinson. The Company of Biologists, Cambridge, England.

Kaback, D. B., V. Guacci, D. Barber and J. W. Mahon, 1992 Chromosome size-dependent control of meiotic recombination. Science **256:** 228–232.

King, J. S., and R. K. Mortimer, 1990 A polymerization model of chiasma interference and corresponding computer simulation. Genetics **126:** 1127–1138.

Kleckner, N., 1996 Meiosis: how could it work? Proc. Natl. Acad. Sci. USA **93:** 8167–8174.

Laurie, D. A., 1980 Inter-individual variation in chiasma frequency and chiasma distribution: a study of *Chorthippus brunneus* and man. Ph.D. Thesis, University of Birmingham, Birmingham, UK.

Laurie, D. A., and G. H. Jones, 1981 Inter-individual variation in chiasma frequency and chiasma distribution in *Chorthippus brunneus*. Heredity **47:** 409–416.

Lawrie, N. M., C. Tease and M. A. Hulten, 1995 Chiasma frequency, distribution and interference maps of mouse autosomes. Chromosoma **140:** 308–314.

Lindsley, D. L., and L. Sandler, 1977 The genetic analysis of meiosis in female *Drosophila melanogaster*. Phil. Trans. R. Soc. Lond. Ser. B **277:** 295–312.

Lyon, M. F., 1976 Distribution of crossing-over in mouse chromosomes. Genet. Res. **28:** 291–299.

Mather, K., 1936 The determination of position in crossing-over. I. *Drosophila melanogaster*. J. Genet. **33:** 207–235.

Mather, K., 1937 The determination of position in crossing-over. II. The chromosome length-chiasma frequency relation. Cytologia, Fujii Jubilaei **1:** 514–526.

Mather, K., 1939 Crossing over and heterochromatin in the X chromosome of *Drosophila melanogaster*. Genetics **24:** 413–435.

Moens, P. B., C. Heyting, A. J. J. Dietrich, W. Van Raamsdonk and Q. Chen, 1987 Synaptonemal complex antigen location and conservation. J. Cell Biol. **105:** 93–103.

Moses, M. J., 1980 New cytogenetic studies on mammalian meiosis, pp. 169–190 in *Animal Models in Human Reproduction*, edited by M. Serio and L. Martini. Raven Press, New York.

Nachman, M. W., and G. A. Churchill, 1996 Heterogeneity in rates of recombination across the mouse genome. Genetics **142:** 537–548.

O'Brien, S. J., 1987 *Genetic Maps 1987*. Cold Spring Harbor Laboratory Press, Cold Spring Harbor, NY.

Peters, A. H. F. M., A. W. Plug, M. J. van Vugt and P. de Boer, 1997 A drying-down technique for spreading of mammalian spermatocytes from the male and female germline. Chrom. Res. **5:** 66–71.

Pigozzi, M. I., and A. J. Solari, 1997 Extreme axial equalization and wide distribution of recombination nodules in the primitive ZW pair of *Rhea americana* (Aves, Ratitae). Chrom. Res. **5:** 421–428.

Polani, P. E., 1972 Centromere localization at meiosis and the position of chiasmata in the male and female mouse. Chromosoma **36:** 343–374.

Poorman, P. A., M. J. Moses, M. T. Davisson and T. H. Roderick, 1981 Synaptonemal complex analysis of mouse chromosomal rearrangements. III. Cytogenetic observations on two paracentric inversions. Chromosoma **83:** 419–429.

Rabbits, P., H. Impey, A. Heppell-Parton, C. Langford, C. Tease *et al.*, 1995 Chromosome specific paints from a high resolution flow karyotype of the mouse. Nat. Genet. **9:** 369–375.

Rahn, M. I., and A. J. Solari, 1986 Recombination nodules in oocytes of the chicken, *Gallus domesticus*. Cytogenet. Cell Genet. **43:** 187–193.

Reid, T., A. Baldini, T. C. Rand and D. C. Ward, 1992 Simultaneous visualization of seven different DNA probes by *in situ* hybridization using combinatorial fluorescence and digital image microscopy. Proc. Natl. Acad. Sci. USA **89:** 1388–1392.

Roeder, G. S., 1997 Meiotic chromosomes: it takes two to tango. Genes Dev. **11:** 2600–2621.

Scherthan, H., S. Weich, H. Schwegler, C. Heyting, M. Harle *et al.*, 1996 Centromere and telomere movements during early meiotic prophase of mouse and man are associated with the onset of chromosome pairing. J. Cell Biol. **134:** 1109–1125.

Shaw, D. D., and G. R. Knowles, 1976 Comparative chiasma analysis using a computerised optical digitiser. Chromosoma **59:** 103–127.

Sherman, J. D., and S. M. Stack, 1995 Two-dimensional spreads of synaptonemal complexes from solanaceous plants. VI. High-resolution recombination nodule map for tomato (*Lycopersicon esculentum*). Genetics **141:** 683–708.

Speed, R. M., 1977 The effects of ageing on the meiotic chromosomes of male and female mice. Chromosoma **64:** 241–254.

Stack, S. M., 1984 Heterochromatin, the synaptonemal complex, and crossing over. J. Cell Sci. **71:** 159–176.

Stack, S. M., and L. K. Anderson, 1986 Two-dimensional spreads of synaptonemal complexes from solanaceous plants. II. Synapsis in *Lycopersicon esculentum*. Am. J. Bot. **73:** 264–281.

Stack, S. M., J. D. Sherman, L. K. Anderson and L. S. Herickhoff, 1993 Meiotic nodules in vascular plants, pp. 301–311 in *Chromosomes Today*, edited by A. T. Sumner and A. C. Chandley. Chapman & Hall, London.

Stephens, S. G., 1961 A remote coincidence. Am. Nat. **95:** 279–293.

Sybenga, J., 1975 *Meiotic Configurations*. Springer-Verlag, Berlin.

Sybenga, J., 1996 Recombination and chiasmata: few but intriguing discrepancies. Genome **39:** 473–484.

Sym, M., and G. S. Roeder, 1994 Crossover interference is abolished in the absence of a synaptonemal complex protein. Cell **79:** 283–292.

West, S. C., 1992 Enzymes and molecular mechanisms of genetic recombination. Annu. Rev. Biochem. **61:** 603–640.

West, S. C., 1994 The processing of recombination intermediates: Mechanistic insights from studies of bacterial proteins. Cell **76:** 9–15.

Wu, T.-C., and M. Lichten, 1994 Meiosis-induced double-strand break sites determined by yeast chromatin structure. Science **263:** 515–518.

Zickler, D., 1977 Development of the synaptonemal complex and the "recombination nodules" during meiotic prophase in the seven bivalents of the fungus *Sordaria macrospora* Auersw. Chromosoma **61:** 289–316.

Zickler, D., P. J. F. Moreau, A. D. Huynh and A.-M. Slezec, 1992 Correlation between pairing initiation sites, recombination nodules and meiotic recombination in *Sordaria macrospora*. Genetics **132:** 135–148.

Communicating editor: R. S. Hawley